Molecular Therapy
Original Article

In Vivo Generation of CAR T Cells Selectively in Human CD4$^+$ Lymphocytes

Shiwani Agarwal,[1,4] Julia D.S. Hanauer,[1,4] Annika M. Frank,[2,3] Vanessa Riechert,[1] Frederic B. Thalheimer,[1] and Christian J. Buchholz[1,2,3]

[1]Molecular Biotechnology and Gene Therapy, Paul-Ehrlich-Institut, 63225 Langen, Germany; [2]Division for Medical Biotechnology, Paul-Ehrlich-Institut, Langen, Germany; [3]Frankfurt Cancer Institute, Goethe University, Frankfurt am Main, Germany

T cells modified with CD19-specific chimeric antigen receptors (CARs) result in significant clinical benefit for leukemia patients but constitute a challenge for manufacturing. We have recently demonstrated the *in vivo* generation of CD19-CAR T cells using the CD8-targeted lentiviral vector (CD8-LV). In this study, we investigated the *in vivo* generation of CD4$^+$ CAR T cells using CD4-targeted LV (CD4-LV). Administration of CD4-LV into NSG mice transplanted with human peripheral blood mononuclear cells (PBMCs) led to 40%–60% of human CD4$^+$ lymphocytes being CAR positive while CD8$^+$ cells remained CAR negative. CAR$^+$ T cells displayed a T helper 1 (Th1)/Th2 phenotype, which was accompanied by CD19$^+$ B cell elimination. Intravenous administration of CD4-LV into NSG mice reconstituted with human CD34$^+$ cells induced CAR expression and B cell elimination within 2–3 weeks post-injection. Preclinical analysis in a tumor mouse model revealed that mice administered CD4-LV exhibited faster and superior tumor cell killing compared to mice injected with CD8-LV alone or as a mixture with CD4-LV. Further analysis suggests that CD4$^+$CAR$^+$ cells may outperform CD8$^+$CAR$^+$ cells, especially at a high burden of target antigen, mainly since CD8 cells are more prone to exhaustion. This first description of *in vivo*-generated CD4$^+$ CAR T cells supports their importance for cellular therapy.

INTRODUCTION

In recent years cellular immunotherapy using T cells armed with chimeric antigen receptors (CARs) has proven to be an effective therapeutic remedy for patients with B cell hematological malignancies.[1–3] CARs are composed of an extracellular binding domain, a hinge region, a transmembrane domain, and one or more intracellular signaling domains.[4] There has been an exponential increase in CAR T cell trials with more than 300 ongoing world-wide trials focusing on different aspects such as CAR activity, applying the approach to different tumor types and simplifying the complex process for manufacturing.[5] With the approval of Yescarta and Kymriah by the US Food and Drug Administration (FDA) and European Medicines Agency (EMA), two products have reached the market.

CAR T cells are individualized cell therapy products and thus require extensive and time-consuming manufacturing procedures. Our group has started to explore the possibility of generating human CD19-CAR T cells directly *in vivo* upon the administration of receptor-targeted lentiviral vectors (LVs) that recognize distinct surface markers on target cells for entry.[6] Surface markers on human lymphocytes have been given special attention.[7] As the primary effector cells, due to their cytotoxic capabilities, CD8$^+$ CAR T cells have been in focus for most of the CAR T studies conducted so far. Recently, we have demonstrated the *in vivo* generation of human CD19-CAR T cells with CD8-targeted LV (CD8-LV).[8] This vector uses the human CD8α chain as entry receptor, thus selectively delivering the CAR gene into CD8$^+$ cells. The *in vivo*-generated CD8$^+$ CAR T cells eliminated CD19$^+$ tumor cells in human peripheral blood mononuclear cell (huPBMC)-transplanted NSG mice.[9] In humanized NSG mice reconstituted with human hematopoietic stem cells, CAR T cell generation was slower but accompanied by B lymphocyte elimination, resulting in symptoms reminiscent of a cytokine-release syndrome (CRS) in some mice.[8]

CD4 T cells are known for their helper function and to intrinsically evoke cytolytic activities by enhancing CD8 T cell activity via cytokine production.[10] However, there have also been reports illustrating a direct cytotoxic activity of CD4 T cells in mediating anti-tumoral activity.[11–13] Consequently, upon the successful *in vivo* generation of human CD8$^+$ CAR T cells, we explored the feasibility of targeting the CAR gene to the CD4 subtype with our lentiviral approach. In this study, we demonstrate the *in vivo* generation of CD19-CAR T cells selectively in CD4$^+$ cells by using the CD4-targeted LV (CD4-LV).[14] Surprisingly, humanized NSG mice administered with CD4-LV displayed a fast kinetic of human CAR T cell generation. These CD4$^+$ CAR T cells substantially reduced or even completely eliminated CD19$^+$ cells. In the anti-tumor model, mice administered with CD4-LV displayed a faster kinetic and were superior in clearing tumor cells compared to mice administered with CD8-LV or a

Received 10 January 2020; accepted 7 May 2020;
https://doi.org/10.1016/j.ymthe.2020.05.005.

[4]These authors contributed equally to this work.

Correspondence: Christian J. Buchholz, Molecular Biotechnology and Gene Therapy, Paul-Ehrlich-Institut, Paul-Ehrlich-Strasse 51-59, 63225 Langen, Germany.
E-mail: christian.buchholz@pei.de

mixture of the two vector types. The data suggest that $CD4^+$ CAR T cells are highly relevant for *in vivo* CAR T cell generation.

RESULTS

To evaluate *in vivo* CAR gene delivery into $CD4^+$ lymphocytes, CD19-CAR(CD3ζ) was packaged into CD4-LV, and as a control into CD8-LV (Figure 1A). PBMCs transduced with the vector expressed the CAR selectively in $CD4^+$ cells (Figure 1B), as described recently for a 4-1BB CD19-CAR.[15] These CAR T cells killed $CD19^+$ but not $CD19^-$ cells in a ratio-dependent manner (Figure 1B). Cytolytic activity was accompanied by increased interferon (IFN)-γ release (Figure 1B). To further explore any cytotoxic differences between $CD4^+$ and $CD8^+$ subtypes, we generated three groups of CAR T cells by transduction of PBMCs with CD4-LV, CD8-LV, or a 1:1 mixture (MIX) of both vector types. All groups contained similar amounts of CAR T cells (Figure S1). The cells were then cocultured with Nalm-6 cells at effector-to-target (E:T) ratios of 1:1 (low tumor burden) or 1:10 (high tumor burden) (Figure 1C). In the low tumor burden setup, all of these CAR T cells effectively controlled target cells (Figure 1E). The MIX group displayed a rapid increase in CAR T cell numbers, resulting in the lowest target cell numbers, in contrast to CAR T cells that had been generated with CD4-LV alone (Figures 1D and 1E). Notably, at high tumor burden, a tendency for a higher activity of CAR T cells generated with CD4-LV compared to those generated with CD8-LV or MIX was observed as determined by the level of tumor cells and the increase in CAR T cells (Figures 1D and 1E). Their cytolytic activity was assessed by upregulation of the degranulation marker CD107a. Notably, CAR T cells generated with CD4-LV displayed similar CD107a expression compared to CAR T cells generated with CD8-LV or MIX (Figure S2A). Activation-induced T cell exhaustion has been considered as one of the mechanisms for the lack of CAR T cells persistent in cellular therapy.[16] To test this hypothesis, we analyzed the inhibitory receptor expression on both of the subsets under the different tumor load setup. Indeed, at the high tumor burden we observed the highest dual expression of Tim-3 and Lag-3 on $CD8^+$ CAR T cells (Figure S2B). Additionally, Tim-3 and Lag-3 were readily upregulated on the CD8 subsets already after 3 days of activation in the absence of CAR gene delivery and tumor cells (Figure S3). From this experimental setup, we can hypothesize that $CD4^+CAR^+$ cells may outperform $CD8^+CAR^+$ cells especially under highly activating conditions such as a high tumor burden, since they are then less prone to exhaustion.

To assess the potential of CD4-LV for *in vivo* generation of CAR T cells, NOD (non-obese diabetic)-SCID (severe combined immunodeficiency)-interleukin $2R\gamma^{null}$ ($IL2R\gamma^{null}$) (NSG) mice were transplanted with activated huPBMCs and a day later vector particles were intraperitoneally (i.p.) administered (Figure 2A). Seven days after vector administration, $CD4^+$ T cells had substantially increased in the peritoneal cavity of vector- over control-injected mice. Also in spleen and blood, $CD4^+$ T cells were slightly increased (Figure 2B). Remarkably, 30%–65% of these cells isolated from the peritoneum, spleen, and blood of the vector group were CAR^+ (Figure 2C). CAR expression was only detected in the $CD4^+$ population, thus confirming the high selectivity of the vector (Figure 2C). Remarkably, all of the mice that had received CD4-LV lacked $CD19^+$ cells in the peritoneum, spleen, and blood (Figure 2D). Furthermore, upon characterization of the CD4 phenotype based on Tbet, Gata-3, retinoic acid-related orphan receptor (ROR)γt, and FoxP3 expression in the peritoneal cavity, we determined that $CD4^+CAR^+$ cells consisted of 31%–55% Th1, 26%–50% Th2, 11%–31% Th17, and 0.15%–0.25% of regulatory T cell (Treg) phenotype, whereas the control groups contained 26%–38% Th1, 44%–53% Th2, 15%–20% Th17, and 1%–1.5% Tregs (Figure 2E; Table S1). Thus, there was an increase in Th1 phenotype upon transduction with CD4-LV compared to the control mice. These data illustrate that human $CD4^+$ CD19-CAR T cells can be generated *in vivo* by using CD4-targeted LVs. Notably, these CAR T cells expanded in presence of antigen stimulation and were potent in eliminating $CD19^+$ cells.

To investigate the functional competence of $CD4^+CAR^+$ cells compared to $CD8^+CAR^+$ cells, NSG mice were transplanted with $CD19^+$ luciferase-encoding Nalm-6 cells. Five days later mice were allocated to four different groups based on the luciferase intensities measured by an *in vivo* imaging system (IVIS) for bioluminescence imaging (BLI) followed by injection of activated huPBMCs. One day later, mice were injected intravenously (i.v.) with CD4-LV, CD8-LV, or MIX (Figure 3A). At day 13, three out of seven mice in the CD4-LV vector-treated group displayed near complete tumor remission, with weak luminescence signals remaining in the forelimbs only, while strong luciferase signals were observed in the remaining three groups (Figure 3B). The remaining four mice treated with CD4-LV and two out of four mice in the MIX group reached almost complete tumor remission by day 20. In the CD8-LV-treated mice reduced luciferase signals were detected compared to the control-treated mice. Statistically significant tumor remission was observed already by day 13 for the CD4-LV-treated group, and for the other vector groups by day 20 compared to the control (Figure 3C). Thus, mice treated with CD4-LV exhibited a faster kinetics in anti-tumoral activities compared to the groups having received CD8-LV or MIX.

At the cellular level, all vector-injected animals exhibited increased levels of human $CD3^+$ lymphocytes in blood, spleen, and bone marrow as compared to the control group. Especially in blood, levels further increased from day 14 to 21 (Figure 4A). CAR T cell levels on day 21 were highest in blood of the MIX group, reaching in some particular animals more than 40% $CD4^+$ and also $CD8^+$ CAR T cells (Figures 4B and 4C). In bone marrow, the highest levels of CAR T cells were present in the CD4-LV-treated group at day 14 (Figure 4B). By day 21, CAR^+ T cell levels in these mice had decreased, which correlated well to the decrease in tumor load. In the MIX and CD8-LV groups, in contrast, CAR^+ T cell levels increased from day 14 to day 21, indicating that these animals had not yet reached the maximal anti-tumoral response (Figures 4B and 4C). With respect to tumor cell levels, CD4-LV treatment resulted in complete elimination of $CD19^+$ cells in bone marrow of the hindlimbs already by day 14, which is well in agreement with the reduced luciferase imaging

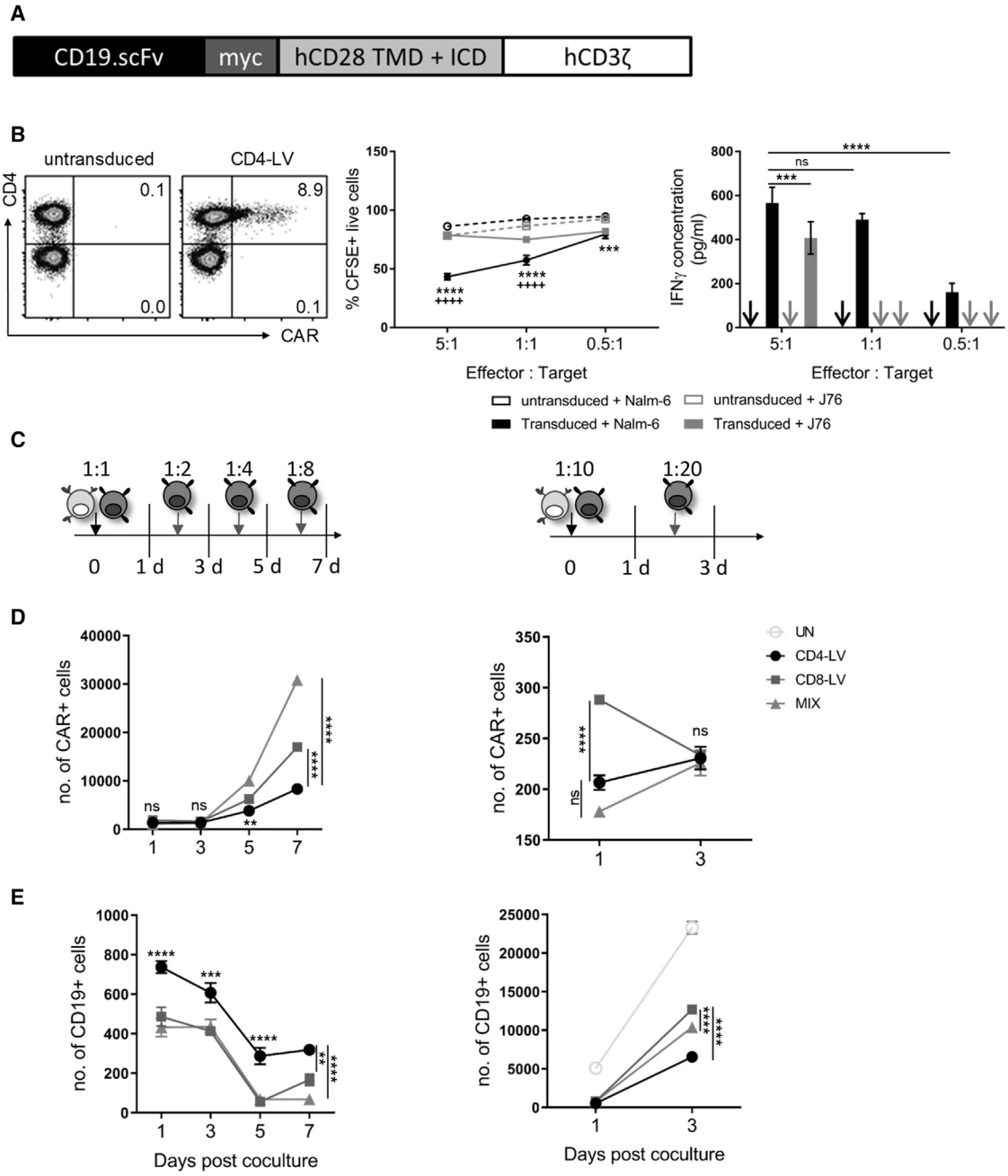

Figure 1. *In Vitro* CAR Delivery by CD4-LV

(A) Graphical representation of the CD19-CAR packaged into CD4-LV. (B) Transduction of human PBMCs with CD4-LV results in exclusive expression of the CAR in $CD4^+$ cells (left panel). CFSE-labeled Nalm-6 and J76 cells were cocultured with transduced or untransduced activated PBMCs at different effector-to-target (E:T) ratios for 24 h (center panel). $CFSE^+$ viable cells were determined by FACS. IFN-γ concentration was determined using ELISA (right panel). (C) Graphical representation of *in vitro* repetitive killing assay with low and high tumor burden. Nalm-6 cells were cocultured with $CD4^+$ or $CD8^+$ or $CD4^+CD8^+$ (MIX) CAR T cells at E:T ratios of 1:1 and 1:10 and rechallenged with a double amount of tumor cells every alternate day. (D and E) The number of CAR^+ cells (D) and tumor cells (E) are enumerated at the denoted time points. Data represent mean ± SEM for all groups; n = 3 of two independent experiments. Statistical significance was determined using two-way ANOVA with Turkey's multiple comparisons test. $^{**}p < 0.01$, $^{***}p < 0.001$, $^{****}p < 0.0001$, comparing different groups to CD4-LV; $^{++++}p < 0.0001$, comparing transduced + Nalm-6 cells to transduced + J76 cells. ns, not significant.

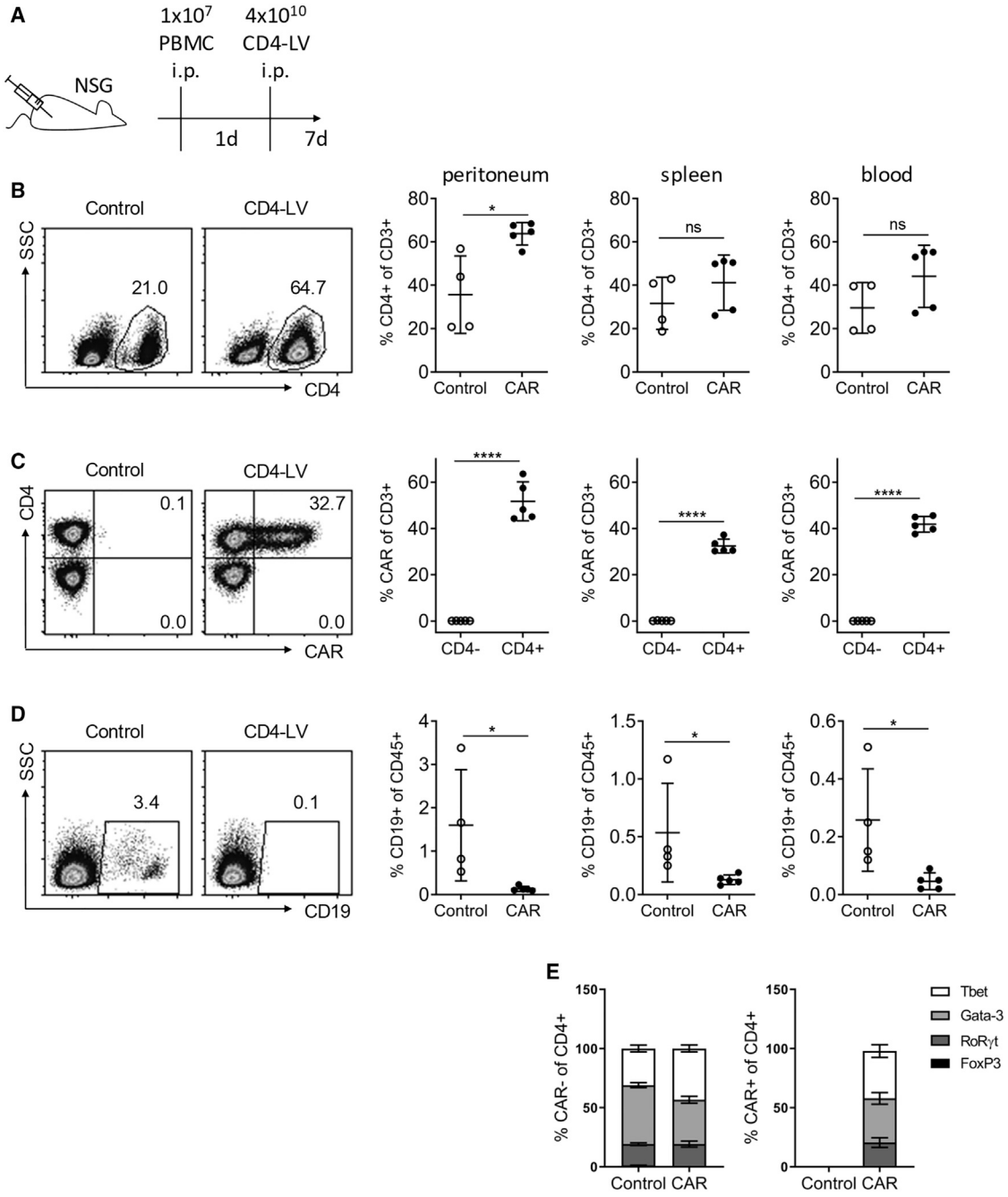

Figure 2. *In Vivo* Generation of CD4$^+$ CD19-CAR T Cells in PBMC-Transplanted Mice

(A) Experimental layout. 1×10^7 *ex vivo*-activated human PBMCs were intraperitoneally (i.p.) injected into naive NSG mice. One day later, the mice were i.p. injected with either PBS (control) or 4×10^{10} particles of CD4-LV encoding for CD19-CAR. Seven days later, mice were sacrificed and organs were harvested. (B–D) Cells isolated from the peritoneal cavity, spleen, and blood were evaluated by flow cytometry for the percentage of CD4$^+$ cells in the CD3$^+$ population (B), CAR$^+$ cells within the CD4$^+$CD3$^+$ and CD4$^-$CD3$^+$ fraction (C), and CD19$^+$ cells within the fraction of human CD45$^+$ cells (D). Representative density plots are shown for cells from the peritoneal cavity. Data represent mean ± SEM for all groups. n = 4 in control group; n = 5 in CD4-LV group. *$p < 0.05$, ****$p < 0.0001$, by an unpaired t test. ns, not significant. (E) Cells isolated from the peritoneal cavity were stained for Tbet, Gata-3, RORγt, and FoxP3 to determine the T cell phenotypes in the indicated cell populations of control and vector groups. Data were adjusted to a total of 100%.

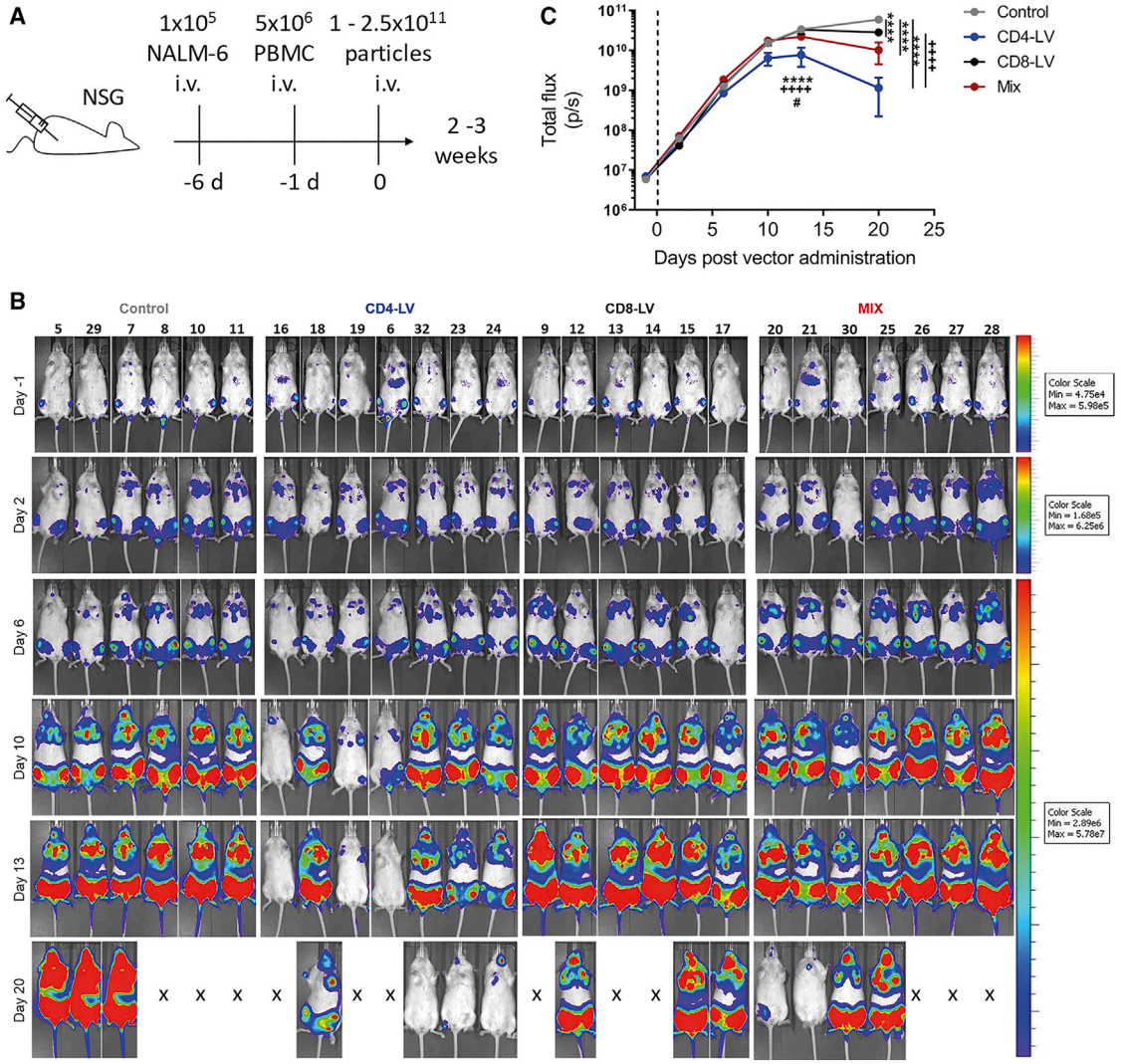

Figure 3. Anti-tumoral Activity of *In Vivo*-Generated CAR T Cells

(A) Experimental layout. 1×10^5 Nalm6-Luc tumor cells were i.v. injected into NSG mice. Five days later, 5×10^6 activated human PBMCs were i.v. administered, and finally a day later the mice were i.v. injected with either PBS (control), or 1×10^{11} particles of CD4-LV, or 2.5×10^{11} particles of CD8-LV, or 5×10^{10} particles of CD4-LV and 1.25×10^{11} particles of CD8-LV (MIX) encoding for CD19-CAR. 14 and 21 days later mice were sacrificed and organs were harvested. (B) Ventral view of all mice included in the experiment recorded at the indicated time points after PBS (control) or vector (CD4-LV, CD8-LV, MIX) administration. Each column represents the bioluminescence imaging (BLI) development of one individual mouse over time. Mice sacrificed at day 14 are indicated by "X" in the day 20 panel. (C) Kinetics of quantified luciferase signals over time is shown as logarithm of the total flux (photons [p]/s). The dotted line indicates the time point of vector administration. Data represent mean ± SEM for all groups (control, n = 6; CD4-LV, n = 7; CD8-LV, n = 6; MIX, n = 7). Statistical significance was determined using a two-way ANOVA with Turkey's multiple comparisons test. $^{****}p < 0.0001$, comparing different groups to control; $^{++++}p < 0.0001$, comparing CD8-LV to CD4-LV; $^{\#}p < 0.05$, comparing MIX to CD4-LV.

data monitored on day 13 (Figures 3B and 4D). Tumor cells having lost CD19 expression were not detected (Figure S5). For the CD8-LV and the MIX groups, a significant reduction of $CD19^+$ cells in bone marrow was documented from day 14 to day 21, while in the same period a substantial increase occurred in the control group (Figure 4D).

To further evaluate the *in vivo* generation of CAR T cells, humanized mice transplanted with human $CD34^+$ hematopoietic stem cells were injected with CD4-LV or MIX. Prior to vector administration the mice received IL-7 to promote T cell activation, thus facilitating lentiviral transduction (Figure 5A). To follow the kinetics of CAR T cell generation, blood was regularly drawn from these mice. Surprisingly, within the second week after CD4-LV administration, mouse #7 displayed 71% CAR^+ cells within the $CD4^+$ lymphocytes in blood (Figure 5B). Six mice showed 2%–12% CAR^+ T cells in blood in the third week after vector injection, whereas mouse #6 contained 0.4% (Figure 5B). In the MIX group, two mice showed similarly high CAR

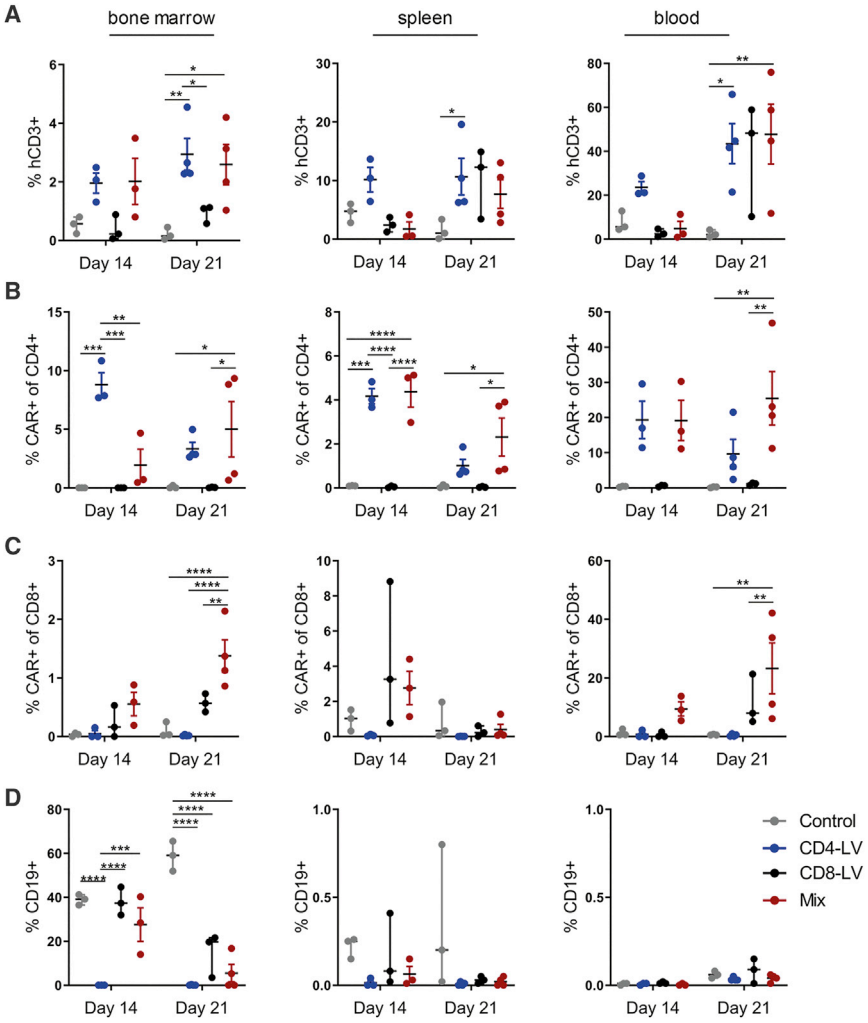

Figure 4. Anti-tumoral Activity at the Cellular Level

(A–D) Cells isolated from the bone marrow, spleen, and blood were evaluated by flow cytometry for the percentage of human $CD3^+$ within the total cells (A), CAR^+ cells in the $CD4^+CD3^+$ (B) and the $CD8^+CD3^+$ fractions (C), and $CD19^+$ cells within total cells (D) at 14 and 21 days after vector administration. The gating strategy is represented in Figure S4. Data represents mean ± SEM for all groups (control, n = 6; CD4-LV, n = 7; CD8-LV, n = 6; MIX, n = 7). Statistical significance was determined using a two-way ANOVA. *p < 0.05, **p < 0.01, ***p < 0.001, ****p < 0.0001.

T cell levels in the $CD4^+$ population (3%–12%) within the third week, and one of the two remaining mice displayed 2% CAR expression in the fifth week. While the $CD4^+CAR^+$ T cells decreased soon after reaching their maximum in the CD4-LV group, they appeared to remain constant in the MIX group (Figure 5B). 10%–28% of $CD8^+$ CAR T cell levels were observed in three out of four mice in the MIX group within the fifth week, whereas no CAR^+ levels were detected in the $CD8^+$ population of mice injected with CD4-LV, thus confirming the high selectivity of the vector (Figure 5C). A strong decrease in $CD19^+$ cell levels, reaching more than 100-fold in some animals, was observed in all mice displaying decent CAR^+ T cell levels (Figure 5D). The only animal exhibiting no significant $CD19^+$ cell reduction over the control group was mouse #4 of the MIX group, which exhibited the lowest CAR T cell levels of all vector-treated animals. Animal #7, which displayed 71% CAR signals in blood, had to be sacrificed about 2 weeks after vector administration due to weight loss, ruffled fur, and hunched posture. The remaining mice developed similar symptoms over time and were sacrificed within 6 weeks after vector administration.

At final analysis, mice administered CD4-LV displayed CAR^+ T cells exclusively in the $CD4^+$ fractions of blood, spleen, and bone marrow (Figure 6A; Figure S6). The MIX group, in contrast, displayed CAR^+ T cells in both the $CD4^+$ and the $CD8^+$ fraction (Figure 6A; Figure S6). Most CAR T cells were present in blood followed by bone marrow and spleen. Because the fluorescence-activated cell sorting (FACS) signals for CAR expression in bone marrow and spleen were relatively weak, we performed cocultivation assays and qPCR to confirm the presence of CAR T cells. After cocultivating splenic cells from these mice with irradiated Raji cells, CAR T cells expanded in samples derived from the CD4-LV group and the MIX group, while splenic cells from control animals did not give rise to any CAR^+ cells (Figure 6B). Notably, samples from animals injected with CD4-LV gave rise to $CD4^+$ CAR T cells only, while samples from the MIX group also contained $CD8^+$ CAR T cells. This confirmed the high level of selectivity in gene delivery reached with CD4-LV. The qPCR performed on genomic DNA isolated from bone marrow confirmed the presence of CAR T cells in the CD4-LV and the MIX groups (Figure 6C). The only exceptions were one mouse from the CD4-LV (#22) and another one from the MIX group (#4). The absence of CAR T cells in mouse #4 thus is well in line with the absence of B cell ablation in this animal.

To determine the activity of *in-vivo*-generated CAR T cells, B cell levels in blood, spleen, and bone marrow of the mice were quantified. In agreement with the monitoring of the levels of CD19 cells over time, all mice of the CD4-LV-injected group exhibited strongly reduced but still detectable $CD19^+$ B cell levels (Figure 6D). The three CAR^+ mice from the MIX group had completely eliminated the B cells not only in blood, but also in bone marrow and spleen. In these organs, B cell levels in the CD4-LV group ranged between 1% and 40% and were thus clearly below those of the control group (Figure 6D).

To assess whether the physical symptoms, such as weight loss, hunched posture, and ruffled fur, observed in $CD34^+$ humanized

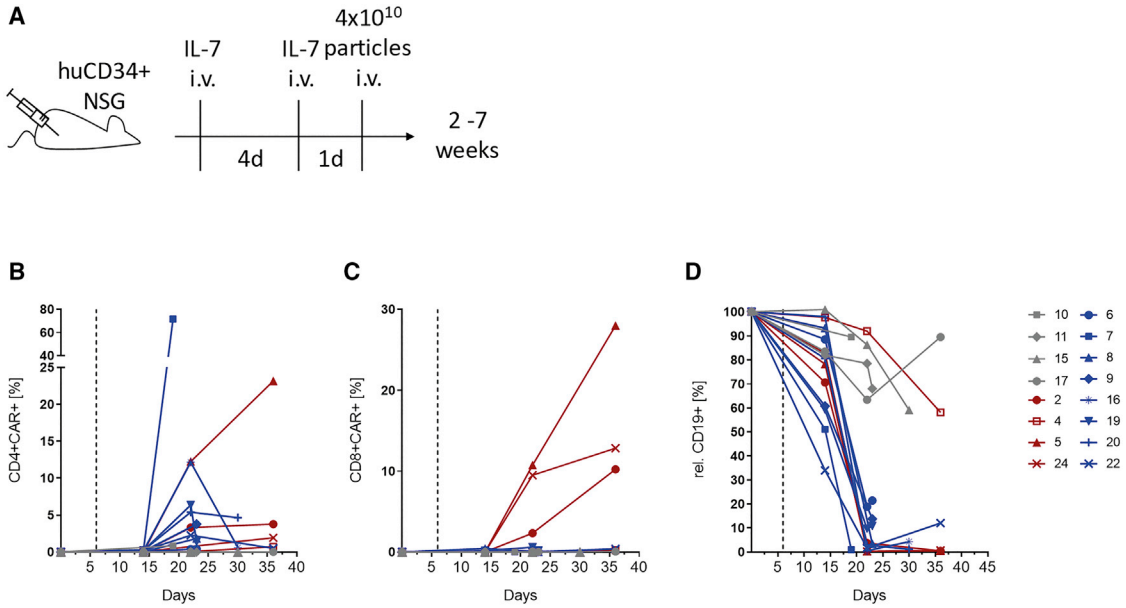

Figure 5. Kinetics of CAR$^+$ and CD19$^+$ Cells in Blood of huNSG Mice

(A) Experimental layout. huNSG mice were injected intravenously twice with IL-7 followed by either PBS (gray lines) or 4 × 10^{10} particles of CD4-LV (blue lines) or 2 × 10^{10} particles of CD4-LV and 3.5 × 10^{11} particles of CD8-LV (MIX) (red lines). (B–D) Cells isolated from the blood over time was evaluated by flow cytometry for the percentage of CAR$^+$ cells in the CD3$^+$CD4$^+$ fraction (B) and the CD3$^+$CD8$^+$ fraction (C) and relative CD19$^+$ cells within the fraction of human CD45 related to the level before vector injection (D) in control, CD4, and MIX groups. The dotted line indicates the time point of vector administration. Distinct symbols used throughout the plots for each individual animal are indicated. n = 4 in the control group; n = 8 in the CD4-LV group; n = 4 in the MIX group.

mice treated with CD4-LV or MIX could be associated with CRS, cytokines were measured in the mouse plasma collected during final analysis. Inflammatory cytokines such as IL-6, IFN-α, granulocyte-macrophage colony-stimulating factor (GM-CSF), and tumor necrosis factor α (TNF-α) were elevated in mice #7 and #19 (Figure S7). An increase in IFN-γ was only observed in mouse #20, which also displayed the highest IL-6 concentration. The MIX mice displayed comparable cytokine concentrations as control mice. Compared to the cytokines levels observed previously in CD8-LV-injected mice,[8] CD4-LV administered mice displayed 2- to 3-fold lower cytokine concentrations. Since histology analysis did not reveal any signs for graft-versus-host disease (GvHD), such as damage to liver portal tracts or intestinal tissue, CRS appears to be the most likely reason for the symptoms in these mice, but will require further investigation.

DISCUSSION

In this study, we describe the successful *in vivo* generation of human CD4$^+$ CAR T cells. So far, it has only been possible to generate CD4$^+$ CAR T cells *ex vivo* upon purification of the cells followed by activation and transduction.[17] Key for our achievement was the vector CD4-LV, which uses CD4 as an entry receptor.[14] Notably, the selectivity of CAR gene delivery into CD4$^+$ cells was very high, if not absolute, since CARs were only detectable in CD8$^+$ cells when the CD8-targeted vector CD8-LV was combined with CD4-LV. By mixing these two vector types in the required ratio, the T cell subpopulations expressing CARs can be precisely controlled and possibly adapted to the patient situation.

We evaluated the *in vivo* CAR T cell generation in immunodeficient mice reconstituted with huPBMCs or CD34$^+$ hematopoietic stem cells. The appearance of CAR T cells was clearly more rapid upon injection of CD4-LV than of CD8-LV in the huPBMC-reconstituted mice. Since *in vivo* it is not possible to determine how many T cells were hit by the vector particles and consequently converted to CAR T cells, we cannot formally exclude that simply more CAR T cells were generated upon CD4-LV injection *in vivo*. The characterization of our vector stocks, however, strongly argues against this possibility. Particle numbers and gene delivery activities of the vector batches used for the *in vivo* experiments show that rather more and definitely not less gene-delivery active vector particles were injected into the CD8-LV groups (see Table S2). However, enhanced tumor cell elimination was substantially more pronounced in CD4-LV- than in CD8-LV-injected mice. A possible explanation for the observed difference could be the T cell phenotypes. Our data show that the generated CD4$^+$ CAR T cells were majorly naive with lower dual inhibitory molecule expression than the corresponding CD8$^+$ CAR T cells, which displayed an effector phenotype with enhanced dual expression of exhaustion markers. At the time of final analysis in the *in vivo* anti-tumoral model, tumor cells were already eliminated in the CD4-LV-injected mice while the anti-tumoral response in the CD8-LV-injected mice was close to or at peak level. It is therefore formally not possible to distinguish whether the difference in exhaustion was causative or a consequence of differences in kinetics. Since this was not only observed *in vivo* but also *ex vivo*, especially in the presence of a high tumor burden, our data rather argue for a principal difference in the exhaustion of CD4$^+$ and CD8$^+$ CAR T cells.

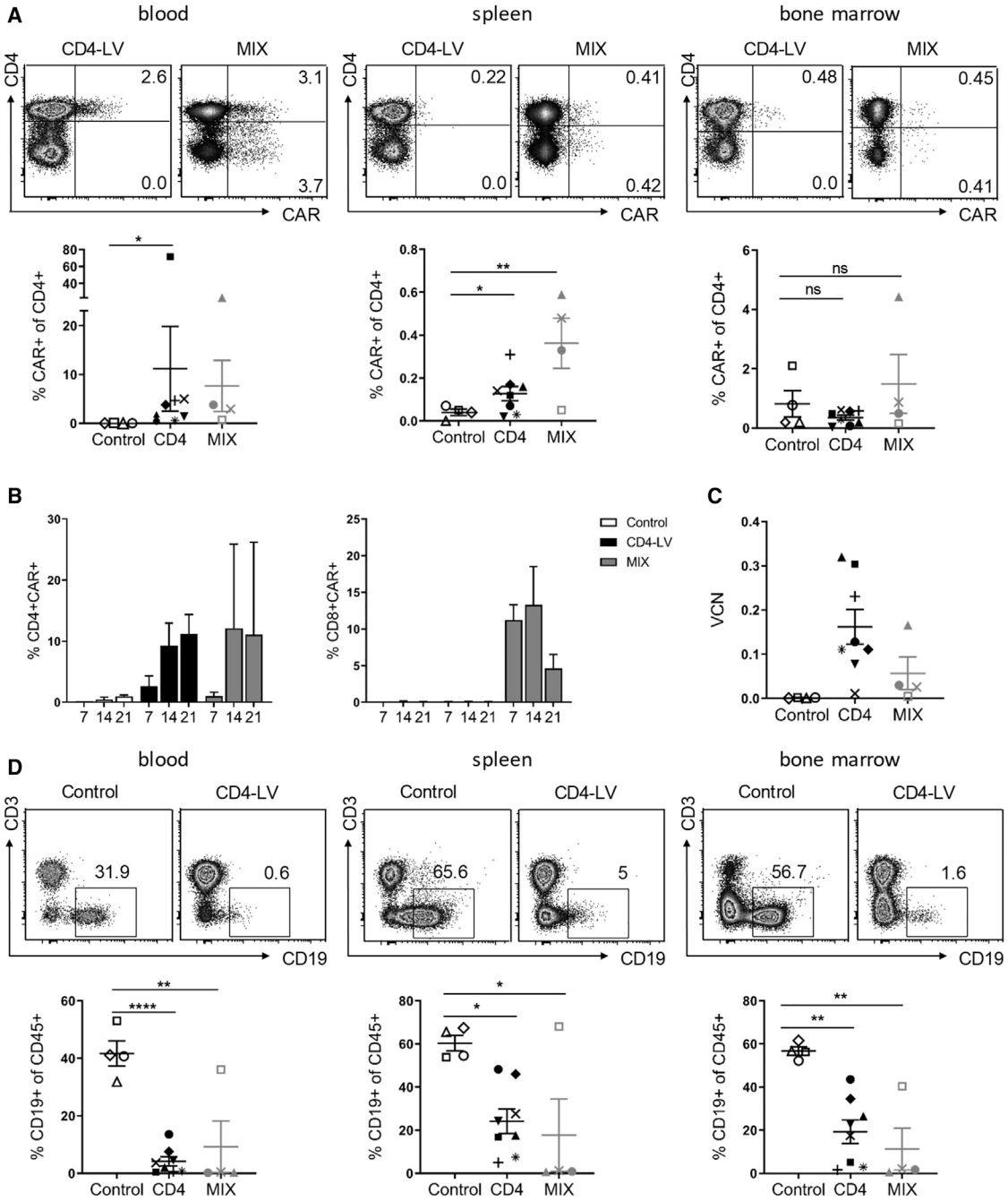

Figure 6. Analysis of Organs from huNSG Mice

Cells isolated from the blood, spleen, and bone marrow were evaluated. Distinct symbols for individual animals are used throughout the plots. Control animals are indicated in open black, whereas vector-treated animals are indicated in filled black (CD4-LV) and filled gray (MIX). (A) Percentage of CAR^+ cells within the $CD4^+CD3^+$ fraction determined by flow cytometry. Representative density plots of one animal from each group at final time point are shown. (B) Splenocytes were cultured with irradiated Raji cells in a 1:1 ratio. On days 7, 14 and 21, CAR T cell levels were determined in the CD4 and CD8 fractions, respectively. (C) Vector copy number (VCN) in genomic DNA isolated from CD4-enriched cells from bone marrow. (D) $CD19^+$ cells within the fraction of human $CD45^+$ cells. Representative density plots of one animal from each group at final time point are shown. Data represent mean ± SEM for all groups. n = 4 in the control group; n = 8 in the CD4-LV group; n = 4 in the MIX group. Statistical significance was determined using a one-way ANOVA. *p < 0.05, ***p < 0.001, ****p < 0.0001. ns, not significant.

This statement is supported by previous data collected *ex vivo* and *in vivo*. By single-cell analysis, it was demonstrated that $CD4^+$ CAR T cells kill target cells but at lower kinetics than $CD8^+$ CAR T cells, while $CD8^+$ CAR T cells are much more prone to activation-induced cell death than are $CD4^+$ CAR T cells, a property that may be more relevant than the killing kinetics *in vivo*.[13] In solid tumor models, CAR T cells face a surplus amount of antigen-positive cells, especially when injected intratumorally. Two independent studies suggest that in such a setting $CD4^+$ CAR T cells are indeed superior over $CD8^+$ T cells since they are less sensitive toward exhaustion.[18,19] With CD19-CAR T cells and hematological tumors, an advantage of $CD4^+$ CAR T cells has been less evident.[17] Indeed, the high amount of systemically injected CAR T cells facing disseminated $CD19^+$ target cells in lymphomas may rather favor the activity of $CD8^+$ CAR T cells.[18] This situation is however different in our setting where CAR T cells are generated upon *in vivo* injection of vector particles. Then, only a few CAR T cells encounter surplus amounts of CD19-positive target cells and suffer stronger exhaustion. Our observations thus support the hypothesis by Wang et al.[18] whereby the injection route determines the ratio of CAR T cells and antigen-positive target cells and thus a potential advantage of $CD4^+$ CAR T cells.

Although the NSG tumor mouse model applied in our study is well established in preclinical analysis of CAR T cells, it is evident that the human lymphocytes in this model are strongly activated due to the xenogeneic reactivity against the mouse tissue. This situation may have favored the expansion of $CD4^+$ CAR T cells owing to T cell receptor (TCR)-mediated activation as well as their higher resistance against activation-induced cell death.[20] In line with this, it has been shown that $CD8^+$ CAR T cells are negatively affected by TCR engagement, causing loss of their effector function due to exhaustion.[21]

In this respect, it is remarkable that $CD4^+$ CAR T cells also exhibited a rapid appearance in the humanized mice where T cells are tolerant against mouse tissue and thus had not experienced activation before CAR gene transfer. Although a side-by-side comparison was not performed, CAR T cells generated *in vivo* with CD8-LV in our previous study[8] appeared roughly 3 weeks later in this mouse model. This faster kinetic of $CD4^+$ CAR T cells, however, came along with only a transient B cell depletion. Interestingly, B cell depletion in this mouse model was permanent when CD8-LV was co-delivered (in this study) or administered alone.[8] This appears to be in contradiction to our *ex vivo* dataset, which revealed that the presence of CD4 T cells augments CD8 T cell proliferation as well as their effector potency. The generation of CAR^+ Tregs by CD4-LV dampening the CD19-targeted immune response could be a potential explanation, which has to be in the focus of future investigation. This holds true also for the signaling domains used in the CAR. We used CD28 in this proof-of-principle study. Interestingly, CAR Treg suppressor functions are especially maintained via CD28 costimulation but not via 4-1BB.[22] Besides Treg activities, CAR T cell persistence is strongly influenced by the chosen signaling domain.[23] Especially a combination of CD28 and 4-1BB or the ICOS-derived signaling domain may substantially enhance the persistence of $CD4^+$ CAR T cells.[24] The selective delivery of CARs into $CD4^+$ cells as demonstrated in our study now allows us to study the properties of $CD4^+$ cells equipped with such advanced CARs directly *in vivo*, thus avoiding any influence from *ex vivo* cultivation conditions.

MATERIALS AND METHODS

Vector Production and Titration

Vector stocks of CD4-LV were produced as described previously.[14] In brief, 0.93 μg of pH-CD4-DARPin (29.2), 4.63 μg of pFcΔ30, 14.4 μg of packaging plasmid pCMVdR8.9, and 15.1 μg of transfer plasmid pS-CD19-CAR-W were cotransfected in 2.5×10^7 HEK293T cells. After 2 days, vector particles released into the supernatant were collected, concentrated, and purified through a 20% sucrose cushion (4,500 rpm, 24 h at 4°C). The supernatant was discarded and the pellet was resuspended in 60 μL of PBS and the vector stocks were stored at −80°C. To determine the gene transfer activity of the vector stocks, A301 cells were transduced with serial dilutions of the vector stock, and CAR^+ cells were quantified by flow cytometry. Similarly, CD8-LV was produced as described in Bender et al.[25] To determine the gene transfer activity in vector stocks, 5-fold dilutions were assayed on Molt4 (CD8-LV) or A301 (CD4-LV) cells. Transducing units (TU) displaying linear correlation with the dilution factor were used for calculations of titers (see Table S2 for details).

Primary Cells and Cell Lines

Human PBMCs were isolated from freshly sampled human blood and were cultured in RPMI 1640 medium (Biowest) supplemented with 10% fetal bovine serum (FBS; Biochrom), 2 mM glutamine (Sigma-Aldrich), 0.5% penicillin/streptomycin, 25 mM HEPES (*N*-2-hydroxyethylpiperazine-*N*′-2-ethanesulfonic acid) (Sigma-Aldrich), and 50 IU/mL IL-2 (Miltenyi Biotec). Prior to activation, PBMCs were depleted for B cells by using human CD19 microbeads (Miltenyi Biotec). For the activation of PBMCs, plates were coated with 1 μg/mL anti-human CD3 monoclonal antibody (mAb) (clone OKT3, Miltenyi Biotec) and 3 μg/mL anti-human CD28 mAb (clone 15E8, Miltenyi Biotec), which were added to the cell culture medium and incubated for 72 h at 37°C, 5% CO_2 and 90% humidity. HEK293T cells were cultivated in DMEM (Gibco) supplemented with 10% FBS and 2 mM glutamine. A301, Molt4, and Nalm-6 were cultivated in RPMI 1640 medium supplemented with 10% FBS and 2 mM glutamine. J76 cells were cultivated in RPMI 1640 medium supplemented with 10% FBS, 2 mM glutamine, 1% non-essential amino acids (NEAAs), and 1 mM sodium pyruvate (NaPyr). All cell lines were regularly tested for mycoplasma using a PCR-based test kit (PanReac AppliChem, Germany). The identity of Nalm-6 was confirmed by genetic phenotyping performed by the German Cell Culture Collection (DSMZ).

Selective Gene Transfer of $CD4^+$ Lymphocytes

Activated PBMCs (4×10^4 cells) were seeded per well in a 96-well plate. 5 μL of CD4-LV was added to the cells, and spinfection was performed by centrifuging at $850 \times g$ for 90 min at 32°C. Fresh medium was added and cells were cultured at 37°C, 5% CO_2 and 90%

humidity. Four days post-transduction, the percentage of CAR^+ cells was determined by flow cytometry.

For evaluating *in vivo* gene transfer, NSG mice (NOD.Cg.*Prkdc*^{scid}*IL2rg*^{tmWjl}/SzJ, Jackson Laboratory) were i.p. injected with 1×10^7 activated human PBMCs followed by i.p. injection of CD4-LV or control. (See Table S2 for details.) Seven days after vector application, mice were sacrificed and the organs (blood, peritoneum, spleen) were harvested for single-cell suspensions, which were further analyzed by flow cytometry.

Humanized $CD34^+$ cord blood-engrafted mice were purchased from Jackson Laboratory. Human $CD45^+$ cells were quantified in the blood by flow cytometry prior to the start of the experiment, and animals were randomly allocated to the vector and control groups, respectively. Mice were i.v. injected with 200 ng of human IL-7 twice, 5 days and 1 day before i.v. injections of 4×10^{10} particles of CD4-LV or 2×10^{10} particles of CD4-LV and 3.5×10^{11} particles of CD8-LV (MIX). Mice were regularly monitored for their weight and health status. CAR expression was determined in the blood of the mice weekly. Once the termination criteria were met, mice were sacrificed and cells from blood, spleen, and bone marrow were harvested to perform flow cytometry analysis. Additional organs were collected and fixed in 4% formalin for histology.

For evaluating *in vivo* anti-tumoral activity, NSG mice were i.v. injected with 1×10^5 Nalm6-Luc cells. A day prior to vector application, bioluminescence imaging was performed to arrange the groups based on luciferase signal intensities followed by i.v. injection of 5×10^6 activated human PBMCs. Finally, the mice were i.v. injected with either control or 1–2.5 $\times 10^{10}$ particles of CD4-LV or CD8-LV or MIX encoding for CD19-CAR. Furthermore, to follow up tumor progression, 2, 6, 10, 13, and 20 days after vector application bioluminescence imaging was performed. In brief, mice were i.p. injected with D-luciferin (PerkinElmer), 150 μg/g body weight, and put into isoflurane anesthesia. The luciferase signals were obtained by bioluminescence imaging using an IVIS (PerkinElmer) 10 min after luciferin injection. Mice were regularly checked for their health status and sacrificed when termination criteria had been reached. 10 days after vector application, mice were bled through the retro-orbital complex to check for circulating CAR T cells in the blood. 14 and 21 days after vector application, blood was taken, mice were sacrificed, and spleen and bone marrow were removed. Animal experiments were performed in accordance with the regulations of the German Animal Protection Law and the respective European Union guidelines. Human blood was provided by anonymous donors in accordance with the rules of the local Ethics Committee.

Preparation of Single-Cell Suspension and Flow Cytometry Analysis

Blood, spleen, and bone marrow were collected from each mouse. Single-cell suspensions of spleen were obtained by mincing the organ through a 70-μm cell mesh. Erythrocytes were lysed by resuspending splenocytes in BD lysis buffer. Bone marrow single-cell suspensions were obtained by flushing the bones with a 23G syringe containing RPMI 1640 medium. The cell suspension was passed through a 70-μm cell mesh and erythrocytes were lysed by resuspending cells in BD lysis buffer. The following antibodies were used for FACS staining: CD45 (2D1, Brilliant Violet [BV]510, BioLegend), CD3 (BW264/56, peridinin chlorophyll protein [PerCP], Miltenyi Biotec), CD4 (RPA-T4, phycoerythrin [PE]-CF594, BD Biosciences), CD8 (BW135/80, fluorescein isothiocyanate [FITC], Miltenyi Biotec), CD62L (DREG-56, BV605, BioLegend), CD45RA (HI100, BV421, BioLegend), CD19 (HIB19, Alexa Fluor 700, Thermo Fisher Scientific), Myc (9B11, PE, Cell Signaling Technology) PD-1 (PD1.3.1.3, PE-Vio 770, Miltenyi Biotec), Lag-3 (REA351, VioBlue, Miltenyi Biotec), Tim-3 (REA635, allophycocyanin [APC], Miltenyi Biotec), CD25 (4E3, PE, Miltenyi Biotec), CD69 (FN50, FITC, Dako), T-bet (O4-46, BV421, BD), Gata3 (L50-823, PE-Cy7, BD Pharmingen), RORγt (Q21-559, Alexa Fluor 647, BD Pharmingen), and FoxP3 (259D/C7, PE-CF594, BD). To determine the viability, fixable viability dye (eFluor 780, Thermo Fisher Scientific) was used. For performing intranuclear staining, a transcription factor buffer set (BD Pharmingen) was used. FACS analysis was performed by LSR II or LSRFortessa (BD Bioscience), and data was analyzed using FCS Express v6 (De Novo Software) or FlowJo v10.1. A percentage of human cells was identified as a living single lymphocyte population that expresses CD45. Cells within the CD45 gate were further gated for CD3 and CD19 populations. Cells within the CD3 gate were gated for human CD8 and CD4 cells. Furthermore, from the CD3, CD4, or CD8 gate, CAR^+ cells were gated and further phenotypic characterization was performed by gating on CAR^+ populations in the different vector groups (see Figure S4 for gating strategy for the tumor model).

Vector Copy Number (VCN)

VCN was determined on genomic DNA, isolated from bone marrow-derived enriched $CD8^+$ and $CD4^+$ T cells of humanized NSG (huNSG) mice using the DNeasy blood and tissue kit (QIAGEN) following the manufacturer's protocol. $CD8^+$ and $CD4^+$ enrichment was performed using CD4 (VIT4, APC) or CD8 (BW135/80, FITC) antibodies together with anti-APC or anti-FITC MicroBeads (all Miltenyj Biotec) following the manufacturer's MS column protocol, respectively. Quantification was performed by a TaqMan-based qPCR assay using the LightCycler 480 Probes Master, the LightCycler 480 Instrument II, and the appropriate LightCycler software for data analysis (all Roche). Transgene detection was performed using a woodchuck hepatitis posttranscriptional element (WPRE)-specific probe (5′-Cy5-CGCCGCCTGCCTTGCCCGCT-BHQ2-3′) and primers (forward, 5′-CACCACCTGTCAGCTCCTTT-3′, reverse, 5′-GGACGATGATTTCCCCGACA-3′). For internal reference, a human albumin-specific probe (5′-6FAM-ACGTGAGGAGTATTT CATTACTGCATGTGT-BHQ1-3′) and primers (forward, 5′-CAC ACTTTCTGAGAAGGAGAGAC-3′, reverse, 5′-CTTGAATTGAC AGTTCTTGCTAT-3′) were used. Simultaneously on the same plate albumin and WPRE were measured as single reactions for samples as well as for the standard (plasmid) in duplicates (once at 95°C for 5 min; 45 times [95°C for 10 s and 60°C for 40 s]). In each case a linear standard curve was used to calculate the amount of human cells

(albumin) and the vector integration (WPRE). The VCN was then calculated as a ratio (copies WPRE/copies albumin) for human cells carrying the WPRE.

In Vitro Killing Assay

Activated PBMCs were incubated with CD4-LV at an MOI of 2 for 72 h at 37°C. CAR expression and the cell count were determined prior to the killing assay in order to adjust CAR^+ cells as the number of effector cells. Target (Nalm-6) and non-target (J76) cells were labeled with CFSE (5- (and 6-)carboxyfluorescein diacetate succinimidyl ester) (Thermo Fisher Scientific) according to the manufacturer's protocol. CAR T cells were then added to 1×10^4 target or non-target cells, seeded in 96 U-bottom plates in ratios ranging from 5:1 to 0.5:1, and cultivated for 24 h at 37°C. 100 μL of supernatant was collected from the coculture and stored at −80°C to perform ELISA to detect IFN-γ secretion. FACS staining was performed, and the dead cells were excluded by staining with the fixable viability dye Zombie NIR (BioLegend). The percentage of viable target cells was calculated by gating on live cells within the $CFSE^+$ fraction.

Repetitive Killing Assay

PBMCs were isolated and CD3 cells were purified using the human Pan T Cell Isolation Kit (Miltenyi Biotec). After 3 days of activation, PBMCs were transduced with CD4-LV or CD8-LV or MIX, respectively, at an MOI of 2 for 72 h at 37°C. CAR expression and the cell count were determined prior to the killing assay in order to adjust the number of CAR^+ cells as effector cells. 4×10^3 CAR T cells were then added to 4×10^3 or 4×10^4 target (Nalm-6) cells seeded in 96 U-bottom plates in ratios of 1:1 (low tumor burden) and 1:10 (high tumor burden) and cultivated at 37°C for 1 week. Every alternate day the dose of Nalm-6 added to the wells was doubled and the following day FACS staining was performed to check for target cell elimination, CAR T cell proliferation, as well as their phenotype.

Expansion Assay

Splenocytes from huNSG mice treated with CD4-LV or MIX were cocultured with irradiated Raji cells at a 1:1 ratio and the coculture was extended/sustained for 3 weeks. Every week, fresh irradiated Raji cells were added into the coculture. At days 7, 14, and 21 FACS staining was performed and the percentage of CAR^+ cells was determined by gating on $CD4^+myc^+$ and $CD8^+myc^+$ events within the $CD3^+$ fraction.

Cytokine Assay

Plasma was isolated from the blood of mice by two-step centrifugation. First, the tubes were centrifuged at $300 \times g$ for 5 min at room temperature (RT), followed by centrifuging the supernatant at $2{,}000 \times g$ for 5 min. Samples were stored at −80°C until analysis with a MACSPlex Human Cytokine 12 kit (Miltenyi Biotec). Samples were analyzed using MACSQuant Analyzer 10 and MACSQuantify 2.09.

Statistical Analysis

Data was analyzed using the GraphPad Prism 7 software (Graph-Pad, USA). Statistical differences were assessed as indicated by using an unpaired t test and two-way ANOVA test with Turkey's multiple comparison test. Differences were considered significant at $p < 0.05$.

SUPPLEMENTAL INFORMATION

Supplemental Information can be found online at https://doi.org/10.1016/j.ymthe.2020.05.005.

AUTHOR CONTRIBUTIONS

S.A. and J.D.S.H. planned and performed the experiments and analyzed data. S.A. drafted the manuscript. A.M.F. established the expansion assay and helped with humanized mouse experiments. F.B.T. contributed to discussions on experimental designs and supervised experiments. V.R. established the qPCR. C.J.B. initiated and supervised the project, acquired grants, and contributed to writing of the manuscript.

CONFLICTS OF INTEREST

C.J.B is listed as the inventor on patents covering T cell-targeted lentiviral vectors. The remaining authors declare no competing interests.

ACKNOWLEDGMENTS

The authors would like to thank Michael Hudecek (Würzburg) for helpful discussions, Gundula Braun (PEI) for producing vector particles, and Manuela Gallet and Tatjana Weidner (both PEI) for their help with animal experiments. Nalm-6-luc cells were kindly provided by Aditi Dey and Adele Fielding (UCL Cancer Institute, London). This work was supported by grants from the Deutsche Krebshilfe (70112578) and the Federal Ministry of Health (03292364) to C.J.B.

REFERENCES

1. June, C.H., O'Connor, R.S., Kawalekar, O.U., Ghassemi, S., and Milone, M.C. (2018). CAR T cell immunotherapy for human cancer. Science *359*, 1361–1365.
2. Sadelain, M. (2017). Chimeric antigen receptors: a paradigm shift in immunotherapy. Annu. Rev. Cancer Biol. *1*, 447–466.
3. Dotti, G., Gottschalk, S., Savoldo, B., and Brenner, M.K. (2014). Design and development of therapies using chimeric antigen receptor-expressing T cells. Immunol. Rev. *257*, 107–126.
4. Miliotou, A.N., and Papadopoulou, L.C. (2018). CAR T-cell therapy: a new era in cancer immunotherapy. Curr. Pharm. Biotechnol. *19*, 5–18.
5. Hartmann, J., Schüßler-Lenz, M., Bondanza, A., and Buchholz, C.J. (2017). Clinical development of CAR T cells-challenges and opportunities in translating innovative treatment concepts. EMBO Mol. Med. *9*, 1183–1197.
6. Buchholz, C.J., Friedel, T., and Büning, H. (2015). Surface-engineered viral vectors for selective and cell type-specific gene delivery. Trends Biotechnol. *33*, 777–790.
7. Frank, A.M., and Buchholz, C.J. (2018). Surface-engineered lentiviral vectors for selective gene transfer into subtypes of lymphocytes. Mol. Ther. Methods Clin. Dev. *12*, 19–31.
8. Pfeiffer, A., Thalheimer, F.B., Hartmann, S., Frank, A.M., Bender, R.R., Danisch, S., Costa, C., Wels, W.S., Modlich, U., Stripecke, R., et al. (2018). *In vivo* generation of human CD19-CAR T cells results in B-cell depletion and signs of cytokine release syndrome. EMBO Mol. Med. *10*, 9158.
9. Agarwal, S., Weidner, T., Thalheimer, F.B., and Buchholz, C.J. (2019). *In vivo* generated human CAR T cells eradicate tumor cells. OncoImmunology *8*, e1671761.

10. Taniuchi, I. (2018). CD4 helper and CD8 cytotoxic T cell differentiation. Annu. Rev. Immunol. *36*, 579–601.

11. Xhangolli, I., Dura, B., Lee, G., Kim, D., Xiao, Y., and Fan, R. (2019). Single-cell analysis of CAR-T cell activation reveals a mixed T_H1/T_H2 response independent of differentiation. Genomics Proteomics Bioinformatics *17*, 129–139.

12. Turtle, C.J., Hanafi, L.-A., Berger, C., Gooley, T.A., Cherian, S., Hudecek, M., Sommermeyer, D., Melville, K., Pender, B., Budiarto, T.M., et al. (2016). CD19 CAR-T cells of defined $CD4^+$:$CD8^+$ composition in adult B cell ALL patients. J. Clin. Invest. *126*, 2123–2138.

13. Benmebarek, M.-R., Karches, C.H., Cadilha, B.L., Lesch, S., Endres, S., and Kobold, S. (2019). Killing mechanisms of chimeric antigen receptor (CAR) T cells. Int. J. Mol. Sci. *20*, 1283.

14. Zhou, Q., Uhlig, K.M., Muth, A., Kimpel, J., Lévy, C., Münch, R.C., Seifried, J., Pfeiffer, A., Trkola, A., Coulibaly, C., et al. (2015). Exclusive transduction of human CD4+ T cells upon systemic delivery of CD4-targeted lentiviral vectors. J. Immunol. *195*, 2493–2501.

15. Jamali, A., Kapitza, L., Schaser, T., Johnston, I.C.D., Buchholz, C.J., and Hartmann, J. (2019). Highly efficient and selective CAR-gene transfer using CD4- and CD8-targeted lentiviral vectors. Mol. Ther. Methods Clin. Dev. *13*, 371–379.

16. Cherkassky, L., Morello, A., Villena-Vargas, J., Feng, Y., Dimitrov, D.S., Jones, D.R., Sadelain, M., and Adusumilli, P.S. (2016). Human CAR T cells with cell-intrinsic PD-1 checkpoint blockade resist tumor-mediated inhibition. J. Clin. Invest. *126*, 3130–3144.

17. Sommermeyer, D., Hudecek, M., Kosasih, P.L., Gogishvili, T., Maloney, D.G., Turtle, C.J., and Riddell, S.R. (2016). Chimeric antigen receptor-modified T cells derived from defined $CD8^+$ and $CD4^+$ subsets confer superior antitumor reactivity in vivo. Leukemia *30*, 492–500.

18. Wang, D., Aguilar, B., Starr, R., Alizadeh, D., Brito, A., Sarkissian, A., Ostberg, J.R., Forman, S.J., and Brown, C.E. (2018). Glioblastoma-targeted $CD4^+$ CAR T cells mediate superior antitumor activity. JCI Insight *3*, e99048.

19. Adusumilli, P.S., Cherkassky, L., Villena-Vargas, J., Colovos, C., Servais, E., Plotkin, J., Jones, D.R., and Sadelain, M. (2014). Regional delivery of mesothelin-targeted CAR T cell therapy generates potent and long-lasting CD4-dependent tumor immunity. Sci. Transl. Med. *6*, 261ra151.

20. Liadi, I., Singh, H., Romain, G., Rey-Villamizar, N., Merouane, A., Adolacion, J.R.T., Kebriaei, P., Huls, H., Qiu, P., Roysam, B., et al. (2015). Individual motile $CD4^+$ T cells can participate in efficient multikilling through conjugation to multiple tumor cells. Cancer Immunol. Res. *3*, 473–482.

21. Yang, Y., Kohler, M.E., Chien, C.D., Sauter, C.T., Jacoby, E., Yan, C., Hu, Y., Wanhainen, K., Qin, H., and Fry, T.J. (2017). TCR engagement negatively affects CD8 but not CD4 CAR T cell expansion and leukemic clearance. Sci. Transl. Med. *9*, eaag1209.

22. Boroughs, A.C., Larson, R.C., Choi, B.D., Bouffard, A.A., Riley, L.S., Schiferle, E., Kulkarni, A.S., Cetrulo, C.L., Ting, D., Blazar, B.R., et al. (2019). Chimeric antigen receptor costimulation domains modulate human regulatory T cell function. JCI Insight *5*, e126194.

23. Weinkove, R., George, P., Dasyam, N., and McLellan, A.D. (2019). Selecting costimulatory domains for chimeric antigen receptors: functional and clinical considerations. Clin. Transl. Immunology *8*, e1049.

24. Guedan, S., Posey, A.D., Jr., Shaw, C., Wing, A., Da, T., Patel, P.R., McGettigan, S.E., Casado-Medrano, V., Kawalekar, O.U., Uribe-Herranz, M., et al. (2018). Enhancing CAR T cell persistence through ICOS and 4-1BB costimulation. JCI Insight *3*, e96976.

25. Bender, R.R., Muth, A., Schneider, I.C., Friedel, T., Hartmann, J., Plückthun, A., Maisner, A., and Buchholz, C.J. (2016). Receptor-targeted Nipah virus glycoproteins improve cell-type selective gene delivery and reveal a preference for membrane-proximal cell attachment. PLoS Pathog. *12*, e1005641.

YMTHE, Volume *28*

Supplemental Information

In Vivo Generation of CAR T Cells Selectively in Human $CD4^+$ Lymphocytes

Shiwani Agarwal, Julia D.S. Hanauer, Annika M. Frank, Vanessa Riechert, Frederic B. Thalheimer, and Christian J. Buchholz

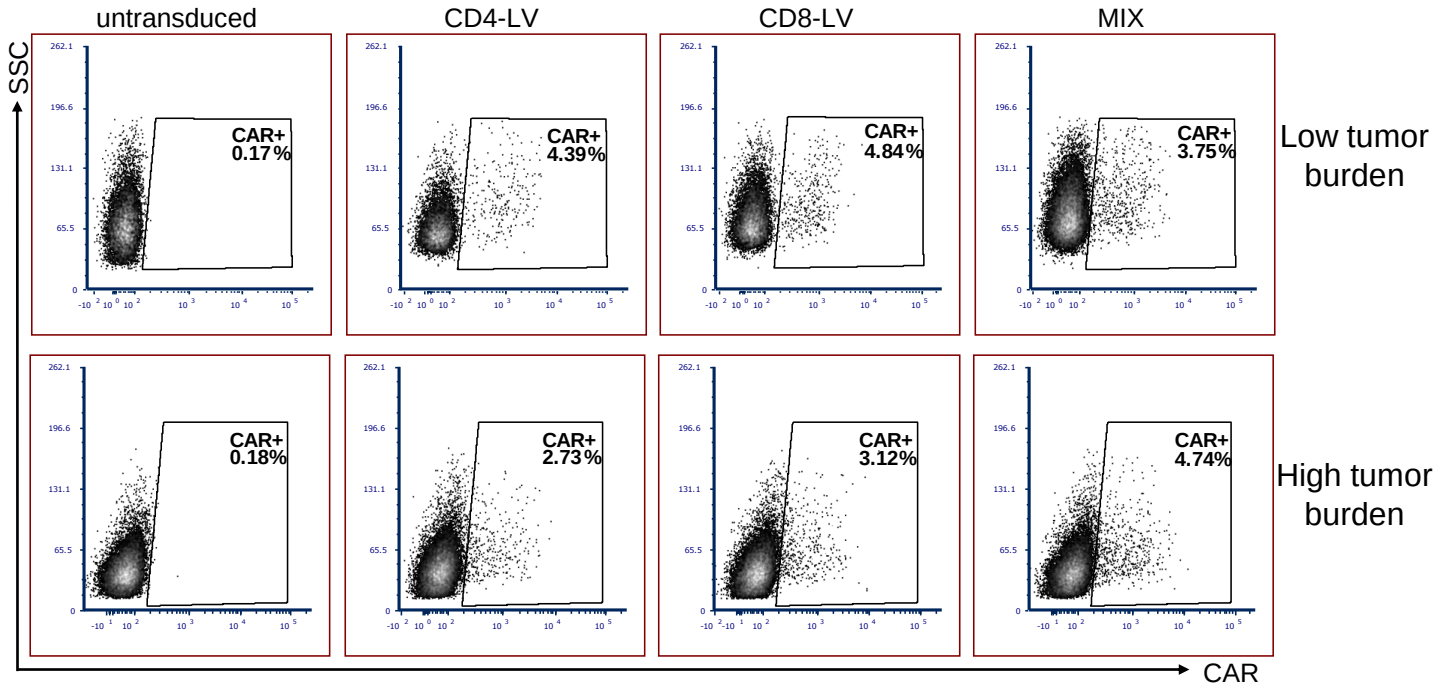

Figure S1: CAR expression at the start of *in vitro* repetitive killing assay

FACS plots displaying CAR expression gated on CD4+, CD8+ and CD3+ populations respectively, analyzed at day 0 of the repetitive killing assay shown in Fig. 1D-E.

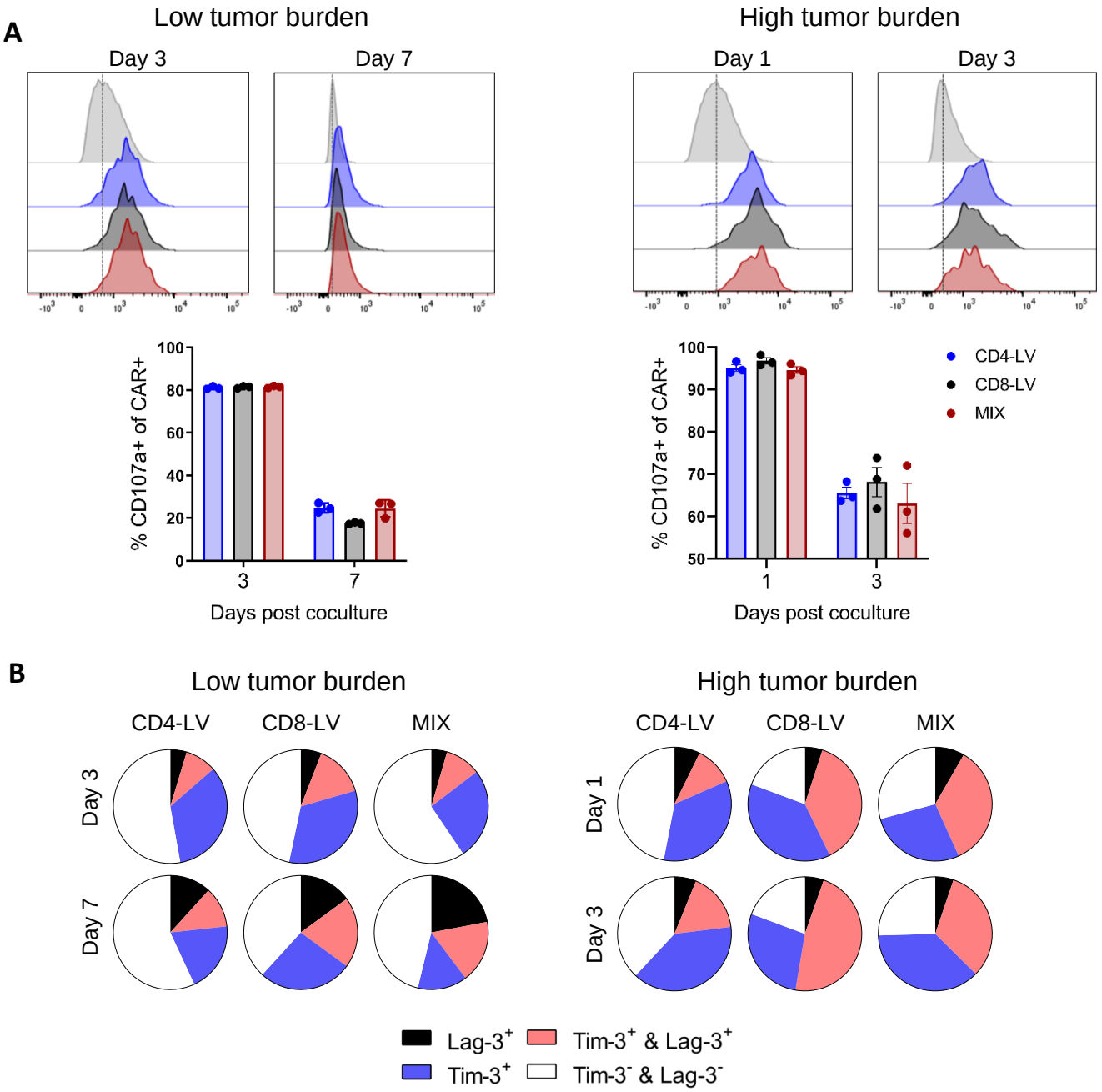

Figure S2: Inhibitory receptor and CD107a expression

(A) Histograms and bar diagrams of CD107a expression and **(B)** graphical representation of inhibitory receptors Lag-3 and Tim-3 on CAR+ T cells gated on CD4+, CD8+ and CD3+ populations respectively, analyzed at day 1, 3 and 7 post coculture of repetitive killing assay of low and high tumor burden (Fig. 1D-E).

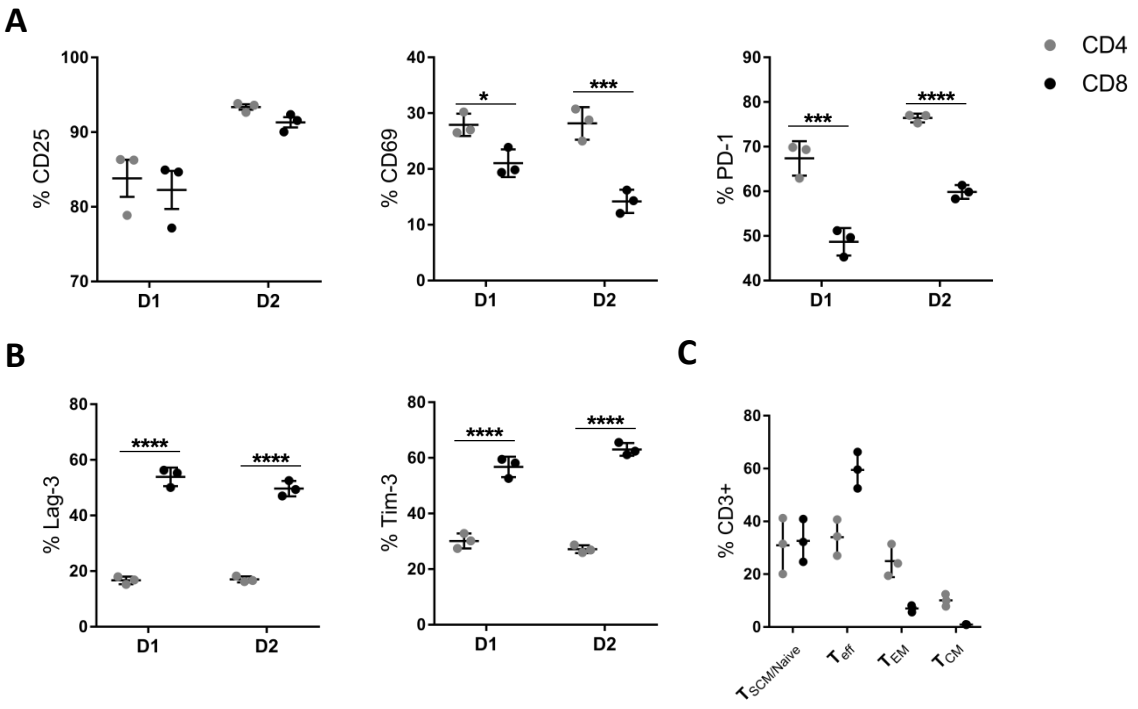

Figure S3: CD8+ T cells display an activation-induced exhausted phenotype

Human PBMC from two donors (D1 and D2) were activated with plate-bound anti-CD3 and anti-CD28 supplemented with IL-2 for 3 days. CD4+ (grey circles) and CD8+ (black circles) fractions were compared for their activation profile based on CD25, CD69 and PD-1 **(A)**, exhaustion profile based on Lag-3 and Tim-3 expression **(B)** and memory phenotype based on CD45RA and CD62L expression **(C)** 3 days post activation by FACS.

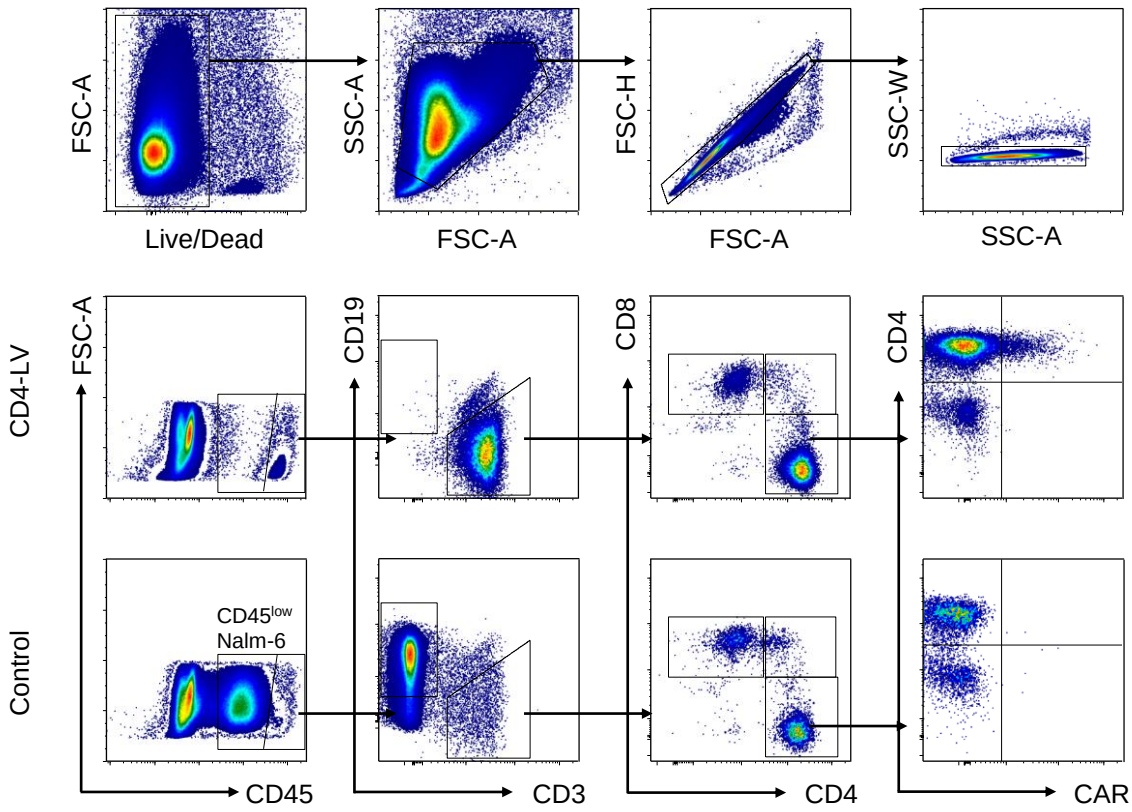

Figure S4: Gating strategy for tumor model

Human cells were identified as living single lymphocyte population that expresses CD45. Cells within the CD45 gate were further gated for CD3 and CD19 populations. Cells within the CD3 gate were gated for human CD8, CD4 and double positive. Further, from the CD4 or CD8 gate CAR positive cells were gated in the different vector groups.

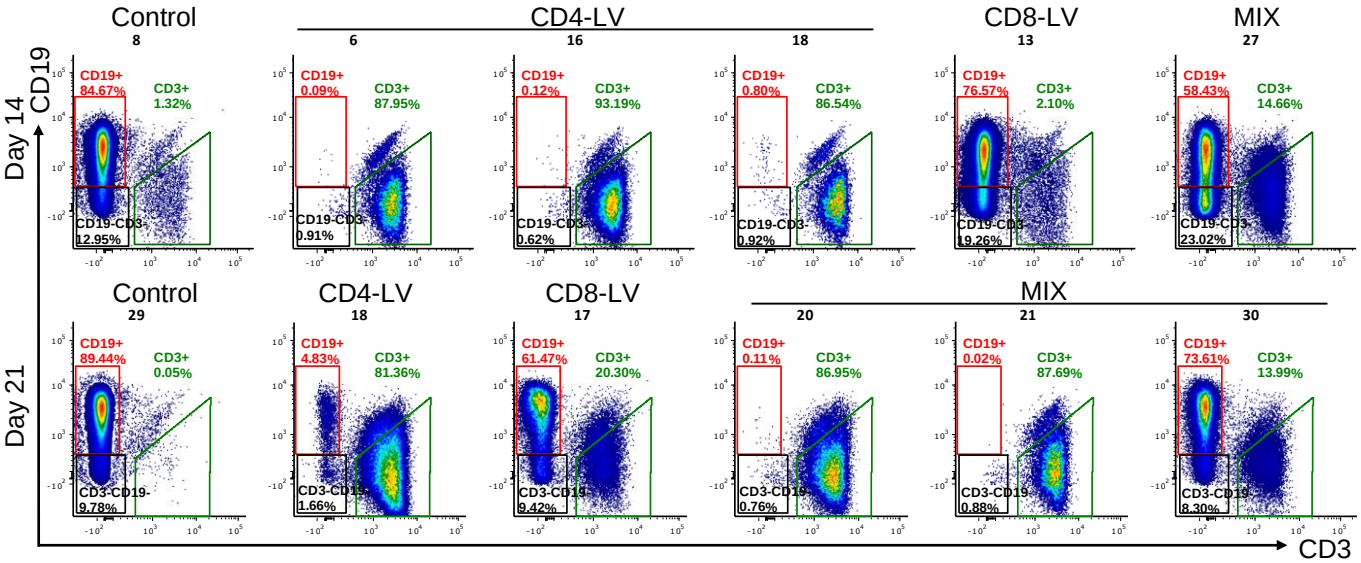

Figure S5: No loss of CD19 expression in Nalm6 cells *in vivo*

Bone marrow cells harvested at day 14 and day 21 from mice of the indicated treatment groups according to Fig. 3 were analyzed by flow cytometry for the presence of CD19-negative Nalm6 cells. Cells were pre-gated on CD45+ population according to Fig. S4. Mice which cleared CD19+ tumor cells (red box) also showed absence of CD3-CD19- cells (black box).

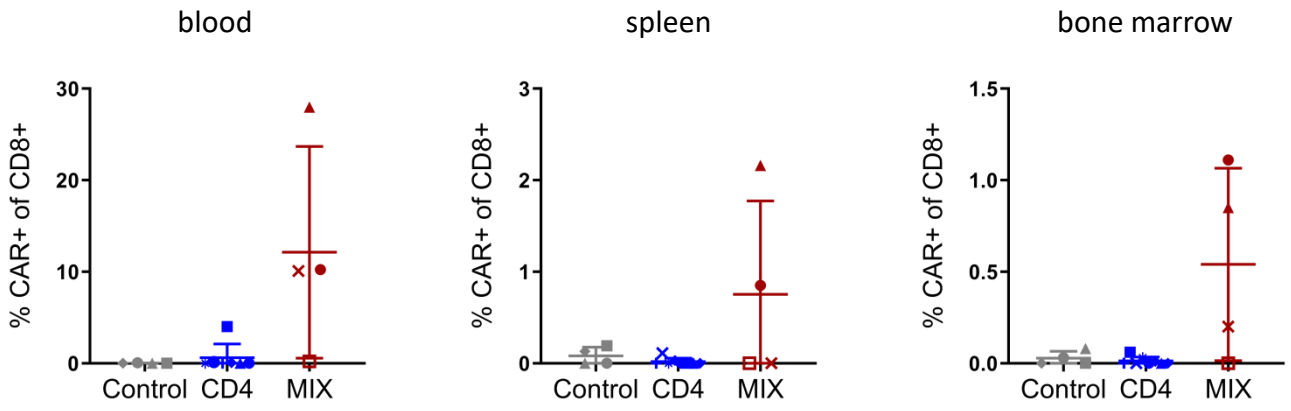

Figure S6: CD8+ CAR T cells in huNSG mice

Cells isolated from the blood, spleen and bone marrow of mice shown in Fig. 5 were evaluated by flow cytometry for the percentage of CAR+ cells within the CD8+CD3+ fraction.

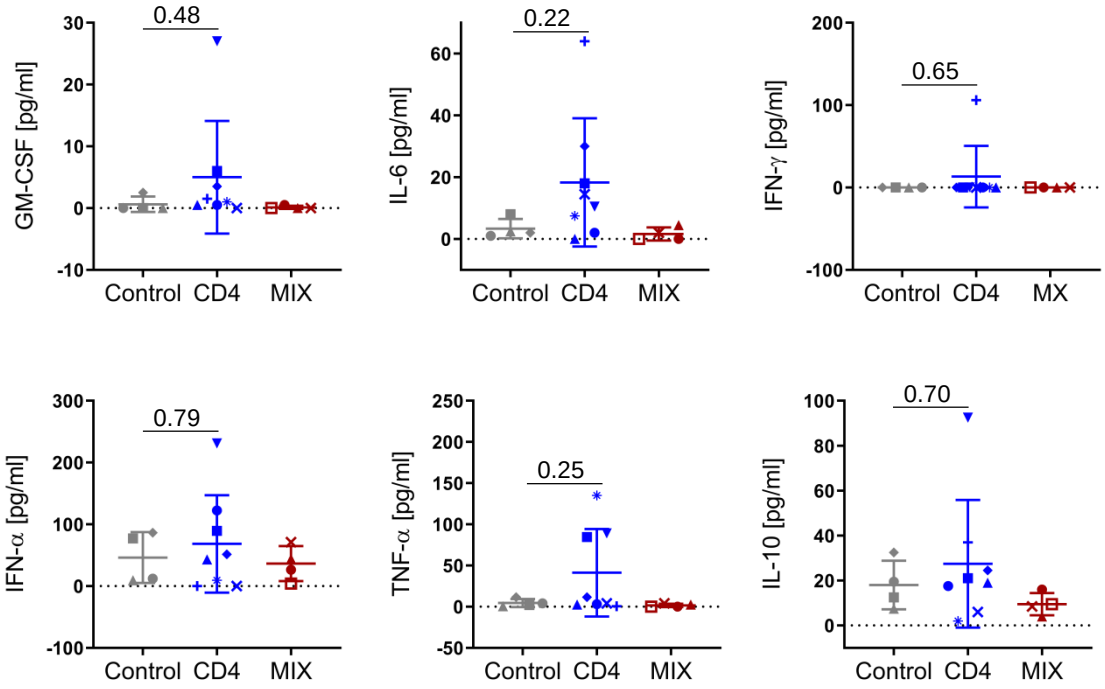

Figure S7: Cytokine levels in humanized mice

Cytokine levels in plasma obtained at final sacrifice of each individual mouse. Every symbol indicates a distinct mouse and is identical to the symbols used in Fig. 5 and 6. Mean ± SEM of n = 2 technical replicates.

Supplemental Table 1: CD4 T cell phenotype

		Tbet (Th1)	Gata-3 (Th2)	RORγt (Th17)	FoxP3 (Treg)
Control	**CD4+CAR-**	30.96 ± 5.72	49.82 ± 4.15	18.01 ± 2.25	1.20 ± 0.22
Vector	**CD4+CAR-**	43.30 ± 6.59	37.47 ± 6.53	18.94 ± 5.83	0.28 ± 0.06
	CD4+CAR+	40.89 ± 12.24	38.16 ± 11.18	20.73 ± 9.15	0.20 ± 0.04

Supplemental Table 2: Vector doses administered *in vivo*

Mice	Experiment	Vector particles injected/mouse		Gene transfer units (t.u.)/mouse	
		CD4-LV	CD8-LV	CD4-LV (A301)	CD8-LV(Molt4)
NSG	Fig. 2	4×10^{10}	-	2×10^{6}	-
	Fig. 3	1×10^{11}	2.5×10^{11}	2×10^{6}	3.6×10^{6}
huNSG	Fig. 5	4×10^{10}	7×10^{11}	2×10^{6}	2.9×10^{6}